Northumbria Research Link

www.northumbria.ac.uk/nrl

northumbria
UNIVERSITY NEWCASTLE

Accepted Manuscript

Thin film solar cells based on the ternary compound Cu_2SnS_3

Dominik M. Berg, Rabie Djemour, Levent Gütay, Guillaume Zoppi, Susanne Siebentritt, Phillip J. Dale

Please cite this article as: Dominik M. Berg, Rabie Djemour, Levent Gütay, Guillaume Zoppi, Susanne Siebentritt, Phillip J. Dale, Thin film solar cells based on the ternary compound Cu_2SnS_3, *Thin Solid Films* (2012), doi: 10.1016/j.tsf.2012.05.085

Thin film solar cells based on the ternary compound Cu_2SnS_3

Dominik M. Berg[a,+], Rabie Djemour[a], Levent Gütay[a], Guillaume Zoppi[b], Susanne Siebentritt[a], Phillip J. Dale[a]

[a] University of Luxembourg, Laboratory for Photovoltaics, 41, rue du Brill, L-4422 Belvaux, Luxembourg
[b] Northumbria University, Northumbria Photovoltaics Applications Centre, Ellison Building, Newcastle upon Tyne, NE1 8ST, UK
[+] current address: University of Delaware, Institute of Energy Conversion, 451 Wyoming Road, Newark, DE 19716, USA, email: berg@udel.edu; Tel.: +1-302-831-3778

Abstract

Alongside with Cu_2ZnSnS_4 and SnS, the p-type semiconductor Cu_2SnS_3 also consists of only Earth abundant and low-cost elements and shows comparable opto-electronic properties, with respect to Cu_2ZnSnS_4 and SnS, making it a promising candidate for photovoltaic applications of the future. In this work, the ternary compound has been produced via the annealing of an electrodeposited precursor in a sulfur and tin sulfide environment. The obtained absorber layer has been structurally investigated by X-ray diffraction and results indicate the crystal structure to be monoclinic. Its optical properties have been measured via photoluminescence, where an asymmetric peak at 0.95 eV has been found. The evaluation of the photoluminescence spectrum indicates a band gap of 0.93 eV which agrees well with the results from the external quantum efficiency. Furthermore, this semiconductor layer has been processed into a photovoltaic device with a power conversion efficiency of 0.54 %, a short circuit current of 17.1 mA/cm^2, a open circuit voltage of 104 mV hampered by a small shunt resistance, a fill factor of 30.4 %, and a maximal external quantum efficiency of just less than 60 %. In addition, the potential of this Cu_2SnS_3 absorber layer for photovoltaic applications is discussed.

1. Introduction

Research of thin film solar cells based on p-type compound semiconductor absorber layers has mainly focused on $Cu(In,Ga)(S/Se)_2$ (CIGS) and CdTe. Recently, $Cu_2ZnSn(S/Se)_4$ (CZTS) has also been considered as a possible candidate for photovoltaic applications since it only consists of abundant elements. However, potentially other p-type semiconductors with fewer elements and perhaps reduced complexity than CZTS are also available such as the ternary Cu-Sn-S system or SnS [1]. In 1987, Kuku and Fakolujo reported on the only previous device, based on a Schottky junction consisting of Cu_2SnS_3 (CTS) and Indium, with a power conversion efficiency of 0.11 % under 100 mW/cm^2 incident radiation [2, 3]. Experimentally, an absorption coefficient of 10^4 cm^{-1} (at energies right above the band gap) [2-5], an electrical conductivity of 10 Ω^{-1}cm^{-1}, a hole mobility of 80 cm^2/(Vs), and a hole concentration of 10^{18} cm^{-3} have been measured for a Cu_2SnS_3 phase [6]. While the absorption coefficient is in the same order of magnitude as those of CZTS and CIGS solar cells, the hole

mobility and electrical conductivity measured by Avellaneda et al. for CTS seem to be a slightly higher than in the case of CZTS and CIGS thin films [6-10]. A possible explanation for these high values was given due to the presence of $Cu_{2-x}S$ phases in those thin films. Apart from these properties, the band gap of the p-type semiconductor Cu_2SnS_3 has been reported to be between 0.93 and 1.51 eV [2-6, 11, 12], which lies in an optimal region for photovoltaic application. While the band gap value of 1.51 eV measured by Kuku et al. appears to be very high, values between 0.93 and 1.35 eV for the band gap seem to be dependent on the crystal structure of the polymorphic compound Cu_2SnS_3, where 0.98 eV was measured for a cubic phase and 1.35 eV for a tetragonal phase [11]. The polymorphic state of a grown Cu_2SnS_3 is dependent on the growth temperature, where the cubic Cu_2SnS_3 is known to form at high temperatures (> 775 °C) and the monoclinic and triclinic as well as the tetragonal phases are low temperature phases (< 775 °C) [13, 14].

For this work, the samples have been prepared at temperatures where a monoclinic or triclinic phase can be expected. To prevent the sample from loosing Sn during the annealing step, which has been reported by Weber et al. [15], the samples have been annealed in a sulfur and tin sulfide containing environment since it has been shown that such an annealing method prevents CZTS layers from losing tin [16].

The focus of this work is two-fold. Firstly, we present structural, compositional, and optical properties of a monoclinic Cu_2SnS_3 thin film prepared by an electrodeposition (ED) method and a subsequent annealing, and secondly we demonstrate the fabrication of thin film solar cell devices based this material and report its opto-electronic properties.

2. Experimental details

The fabrication of the absorber layer was carried out in a two step process. At first, Cu and Sn were sequentially electrodeposited in a double sandwich order Mo/Cu/Sn/Cu/Sn from a basic Cu and an acidic Sn bath onto a square 25 x 25 mm^2 Mo-coated soda-lime glass substrates. Details of the ED method as well as the bath compositions and potentials used are given elsewhere [17]. Following the ED, the precursor was then annealed in a tube furnace at 550 °C for two hours at 50000 Pa (500 mbar) in a N_2/H_2 (90/10) atmosphere together with elemental sulfur (99.9995% purity) and SnS (99.5% purity) powder to convert the metal stack into the desired Cu_2SnS_3 compound. Further details of the annealing procedure can be found in [16]. The sample was etched for 30 s in a 5 wt% KCN solution to remove possible copper sulfide phases. Photovoltaic devices were formed by the addition of a chemical bath deposited CdS buffer layer (90 nm), followed by sputtered i-ZnO and Al:ZnO layers, and a Ni:Al front contact grid. Compositional and morphological information of the absorber layer have been gained using energy-dispersive X-ray spectroscopy (EDX: Oxford Instruments INCA X-MAX, using 20 kV acceleration voltage) and scanning electron microscopy (SEM: Hitachi SU-70), respectively, and the phase analysis has been carried out using grazing incidence X-ray diffraction (GI-XRD: Bruker D8; grazing angle of 0.75 °, Cu Kα_{1+2} X-ray source). Photoluminescence (PL) measurements have been performed on a home-built setup at room temperature with an excitation wavelength of 514.5 nm using an argon ion laser, with an incident power of 40 μW, and a spot size of 1 μm^2. The PL signal has been integrated over an area of 20 x 20 μm^2. The solar cell devices were characterized by current density – voltage (JV) measurements using a halogen lamp (100 mW/cm^2) and

the external quantum efficiency (EQE) measurement was carried out on a home-built setup. For both, experimental details can be found in Scragg et al. [17].

3. Results and Discussion

3.1. Precursor

The electrodeposition conditions have been chosen in a way that the metallic layers of the precursor consist of small and densely packed grains to get uniform and homogeneously covering precursors [17]. Figure 1(a) and (b) show SEM images of the metallic Cu layer on Mo and of the Sn layer on the Cu film. In both cases, a rather compact structure could be achieved, with a Cu grain size in the range of 100 nm, whereas the Sn grains reach sizes of around 600 nm. Important for the annealing, and hence for the reaction with sulfur and SnS from the gas phase, is the distribution of the metals in the precursor. We hypothesize that it is preferable for Cu and Sn to be close to each other such that a direct reaction forming Cu_2SnS_3 can be achieved. Therefore, the double sandwich stacking order has been chosen to increase the surface area between the copper and tin. It has been observed by XRD measurements (not shown here) that already at room temperature, within the first 24 hrs after deposition, a Cu/Sn/Cu stack alloys to form a CuSn phase. This pre-alloying supports a direct formation of the Cu_2SnS_3 phase during the process of annealing. The composition of the precursor was chosen to have a slight excess of Sn compared to stoichiometry ([Cu]/[Sn] $\approx$ 1.3).

3.2. Composition and morphology of the absorber layer

Unlike the metallic layers of the precursor, the morphology of the absorber layer, shown in Figure 1 (c) and (d), has a much less compact structure that is homogeneously distributed over the whole surface area of the sample. Large grains of between 2 and 6 μm in diameter can be observed with pinholes of similar horizontal dimensions. All together it was found that 67.5 % of the average sample's surface is covered with grains, leaving a third with pinholes. The effect that leads to such a morphology is yet unclear, but might be connected to the annealing strategy used. The grains shown in Figure 1 (c) and (d) appear to be single phase, however an EDX compositional analysis of a single grain after KCN etching shows a Cu/Sn ratio of 1.9 and a S/(Cu+Sn) ratio of 1.09. These values are slightly S rich and Cu poor with respect to a stoichiometric Cu_2SnS_3, therefore secondary Sn rich phases cannot be excluded.

3.3. Structural Investigations

Figure 2 shows the diffractogram as obtained by GI-XRD measurements. Apart from the peaks marked with a red or green arrow, all other experimental peaks could be assigned to the monoclinic Cu_2SnS_3 phase (JCPDS: 04-010-5719, see blue vertical lines), which was discussed by Onoda et al. [13]. This phase is also the expected one at the used annealing temperature of 550 °C [13]. The marked peaks (red or green arrows) could be assigned to Mo (red) and MoS_2 (green). The fuzzy broad peak of MoS_2 at around 34 ° is rather dominant, which is mainly due to the large surface area of pinholes on the sample. The majority phase of this sample however can clearly be attributed to a monoclinic Cu_2SnS_3 phase.

3.4. Opto-Electronic Properties

3.4.1. Absorber layer

Figure 3(a) shows a PL spectrum recorded at room temperature. There, a fairly broad and asymmetric peak at 0.95 eV can be seen, which is attributed to band-band transition, as the peak position is in the same energy range as the band gap value extracted by EQE (see further below). As described by Würfel [18], the PL signal detected can be spectrally described by Planck's generalized law

$$Y_{PL}(E) = \frac{1}{4\pi^2 \hbar^3 c^2} \frac{a(E)E^2}{\exp((E - \Delta\mu)/k_B T) - 1}$$

where the absorptivity is given by $a(E) = (1 - R_f)(1 - \exp(-\alpha(E)d))$ with the front surface reflectivity R_f, the absorption coefficient $a(E)$, the layer thickness d, the temperature T, the energy E, and where $\Delta\mu$ is the quasi-Fermi level splitting. For PL which occurs from band-band transition, the high energy wing of the measured spectrum can be fitted to the Bose-term in this equation. Furthermore, a good fit at photon energies above the band gap, respectively, confirms that the involved charge carriers are thermally relaxed quasi-free carriers in the band. In a next step of the evaluation the absorptivity of the emitting matter can be extracted, which then usually saturates to 1 for photon energies above the band gap. This is only observed if the fit of the Bose-term in the previous step is good enough and if the active layer is thick enough to reach an absorptivity of 1. More details about this evaluation procedure can be found in [19].

In the insert in Figure 3(a) we show the extracted spectral absorptivity which saturates to unity for photon energies > 0.97 eV. From the shown absorption edge we extract a value for the optical absorption threshold by intercepting the graph at $a(E) = 1/e$, as described in [19]. We interpret this value to correspond to the optical band gap of the material, which gives $E_G = 0.93$ eV.

Following the procedure described in [20], furthermore an absorption coefficient has been extracted which amounts to $\alpha > 10^4$ cm^{-1} for photon energies > 0.95 eV (slightly higher energy than the band gap). This number reflects only a rough estimate for the absorption coefficient as a few assumptions had to be made for the evaluation: In principle this evaluation is based on the considerations stated above and a thickness of 1 μm for the absorber layer. This value was measured from SEM cross sections (see Figure 1(d)) and is an upper estimate for d. Thus, as the evaluation of the absorption coefficient from the absorptivity follows basically the invers Beer-Lambert law our found values for alpha are merely a lower estimate for α. Nevertheless, our results for alpha along with the value for E_g lie within the range of what has been reported in literature [5, 6].

3.4.2. Photovoltaic device

Figure 3(b) shows the solar cell performance of the best device obtained from this monoclinic ternary compound. The dashed line represents the JV curve in the dark and the solid one the JV curve under illumination. The open-circuit voltage (V_{OC}) is 104 mV, the short-circuit current (J_{SC}) is 17.1 mA/cm^2, the fill factor (FF) is 30.4 %, and the power conversion efficiency is 0.54 %. The reason for the small J_{SC} is due to the fact that only

two thirds of the sample's surface have been covered with the absorber layer. Therefore, only two thirds of the photons arriving at the surface can be maximally absorbed. Furthermore, a large size and quantity of the pinholes could also cause the shunt resistance ($R_{sh} = 23 \, \Omega cm^2$) to be this small. This latter value has been obtained by fitting the negative potential side of the dark JV curve, while the serial resistance (R_S) has been obtained by plotting the high potential side. R_S has been found to be $2.0 \, \Omega cm^2$. The values presented here belong to the best cell measured, however in total six functional devices, each having a conversion efficiency of larger than 0.27 % (V_{OC} ranging between 80 and 104 mV, and J_{SC} ranging between 11 and 17.1 mA/cm^2), have been made so far. Hereby, the overall low V_{OC} might be related to a high charge carrier recombination in the device. Up to this point, however, there have been no further attempts to optimize the efficiencies of such a device.

The EQE of the best device is shown in Figure 3(c), along with an area corrected effective EQE. The area correction assumes all photons to arrive on absorber material. Where the measured EQE shows a maximum value of just less than 60 %, that of the effective EQE is just less than 90 % which is within the range of the highly efficient CIGS solar cells. This shows the high potential of the Cu_2SnS_3 based solar cells. Since the device has not been optimized yet, further reasons for the poor performance could be due to reflections losses at the front of the device, unwanted absorption in the window layer, or a bad charge carrier collection. The device shown here was an initial attempt to make a solar cell device from a Cu_2SnS_3 absorber layer based on a pn-junction.

Calculating the short circuit current by integrating the EQE with the AM1.5 solar spectrum gives a value of $J_{SC,EQE} = 25.07$ mA/cm^2 which is significantly higher than what has been measured in the JV curve ($J_{SC} = 17.1$ mA/cm^2). One reason for this discrepancy can be found in the front grid of the device. This taken into account would lead to a grid corrected short circuit current of $J_{SC,gridcorrected} = 18.23$ mA/cm^2, in comparison to the measured J_{SC} from the JV curve. The further discrepancy to $J_{SC,EQE}$ can be explained by an underestimation of our JV setup for such a low band gap material due to the use of a halogen lamp which not very well matches the solar spectrum. Therefore, one can expect the real efficiency of this device to be even higher than the 0.54 % measured. Calculations of J_{SC} from the effective EQE even lead to a larger value of the short circuit current ($J_{SC,EQEeff} = 37.14$ mA/cm^2). This effective $J_{SC,EQEeff}$ is very high and shall demonstrate the potential of this ternary compound for photovoltaic applications.

Extrapolating the E_G from the EQE, as shown in Figure 3(d), one can see that the absorber layer is either not single phase or that the monoclinic Cu_2SnS_3 phase has two band gaps at 0.93 and 0.99 eV. The lower of the two values fits also nicely to what has been obtained from the PL measurement and to literature values [6, 11].

4. Conclusion and Outlook

In this work, we showed a method to produce a Cu_2SnS_3 thin film semiconductor via the annealing of an electrodeposited precursor in a S and SnS environment. Compositional as well as structural investigations have shown that the majority of the film consists of a monoclinic Cu_2SnS_3 phase. The band gap of this ternary phase has been determined independently from PL and EQE to be at 0.93 eV, where the band gap evaluation from the EQE suggests a second band gap at 0.99 eV. A room temperature PL spectrum shows a peak at 0.95 eV.

Additionally, it has been shown that the ternary Cu_2SnS_3 thin film can be used as an absorber layer in a pn-junction based device. The power conversion efficiency of the device presented in this work was measured to be 0.54 %, which is a factor of five higher than what had been obtained with a Schottky based device before. An external quantum efficiency of less than 60 %, a small J_{SC} of 17.1 mA/cm^2, and a tiny R_{sh} of 23 Ωcm^2 could be explained by a high number of pinholes, leaving only 67.5 % of the sample surface to be covered by Cu_2SnS_3 grains, suggesting that a much higher efficiency could be achieved by a more densely packed absorber layer which was shown in a calculated effective EQE.

Acknowledgement

References and Notes

[1] M. Ristov, G. Sinadinovski, M. Mitreski, M. Ristova, Sol. Energy Mater. Sol. Cells 69 (2001) 17.

[2] T. Kuku, O. Fakolujo, Sol. Energy Mater. 16 (1987) 199.

[3] On first sight, the compound presented by Kuku et al. [2] seems to be very Cu deficient compared to the stoichiometric ratio, however this apparent discrepancy appears to be a labeling error concerning the film composition, meaning that in Table 1 the unit "at.%" probably meant to be "wt.%".

[4] M. Bouaziz, J. Ouerfelli, S. Srivastava, J. Bernde, M. Amlouk, Vacuum 85 (2011) 783.

[5] M. Bouaziz, M. Amlouk, S. Belgacem, Thin Solid Films 517 (2009) 2527.

[6] D. Avellaneda, M. Nair, P. Nair, J. Electrochem. Soc. 157 (2010) D346.

[7] H. Katagiri, N. Ishigaki, T. Ishida, K. Saito, Jpn. J. Appl. Phys. 40 (2001) 500.

[8] S. Siebentritt, Thin Solid Films 480-481 (2005) 312.

[9] D. Schroeder, J. Hernandez, G. Berry, A. Rockett, J. Appl. Phys. 83 (1998) 1519.

[10] D. Mitzi, O. Gunawan, T. Todorov, K. Wang, S. Guha, Sol. Energy Mater. Sol. Cells 95 (2011) 1421.

[11] P. Fernandes, P. Salome, A. Cunha, J. Phys. D: Appl. Phys. 43 (2010) 215403.

[12] S. Fiechter, M. Martinez, G. Schmidt, W. Henrion, Y. Tomm, J. Phys. Chem. Solids 64 (2003) 1859.

[13] M. Onoda, X.-A. Chen, A. Sato, H. Wada, Mater. Res. Bull. 35 (2000) 1563.

[14] D.M. Berg, R. Djemour, L. Gütay, S. Siebentritt, P.J. Dale, X. Fontane, V. Izquierdo-Roca, A. Perez-Rodriguez, Appl. Phys. Lett. 100 (2012) 192103.

[15] A. Weber, R. Mainz, H. Schock, J. Appl. Phys. 107 (2010) 013516.

[16] A. Redinger, D.M. Berg, P.J. Dale, S. Siebentritt, J. Am. Chem. Soc. 133 (2011) 3320.

[17] J. Scragg, D.M. Berg, P.J. Dale, J. Electroanal. Chem. 646 (2010) 52.

[18] P. Würfel, J. Phys. C: Solid State Phys. 15 (1982) 3967.

[19] T. Unold, L. Gütay. In: Advanced Characterization Techniques for Thin Film Solar Cells (D. Abou-Ras, T. Kircharzt, and U. Rau, eds.), WILEY-VCH, (2011).

[20] L. Gütay, C. Lienau, G. Bauer, Appl. Phys. Lett. 97 (2011) 052110.

Figure Caption

Figure 1
SEM images of (a) the Cu layer on the Mo substrate, (b) Sn layer on Cu, (c) the etched absorber layer in top view, and (d) the etched absorber layer in cross sectional view.

Figure 2
GI-XRD pattern of the etched absorber layer together with the peak positions for the monoclinic Cu_2SnS_3. The red and green arrows indicate the contributions of Mo and MoS_2, respectively. The peaks were assigned using the ICDD database (monoclinic Cu_2SnS_3: 04-010-5719, Mo: 04-001- 0059, MoS_2:00-009-0312).

Figure 3
(a) PL peak of the absorber layer and the extracted absorptivity a(E). (b) JV curve of the best solar cell device. (c) EQE (black solid line) and effective EQE (blue dashed line) of the device. (d) Band gap extraction from the EQE.
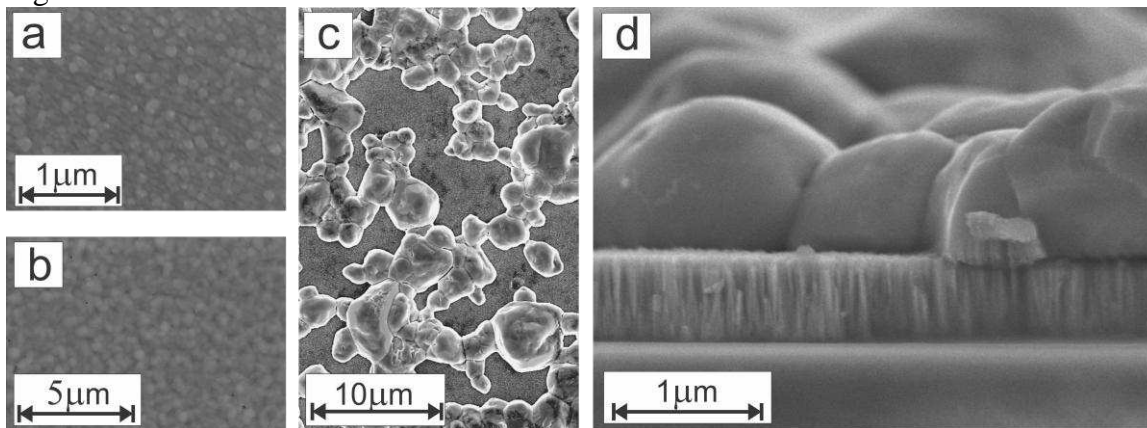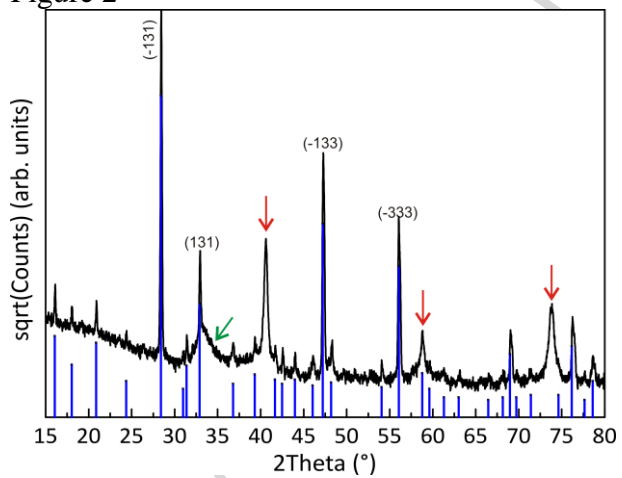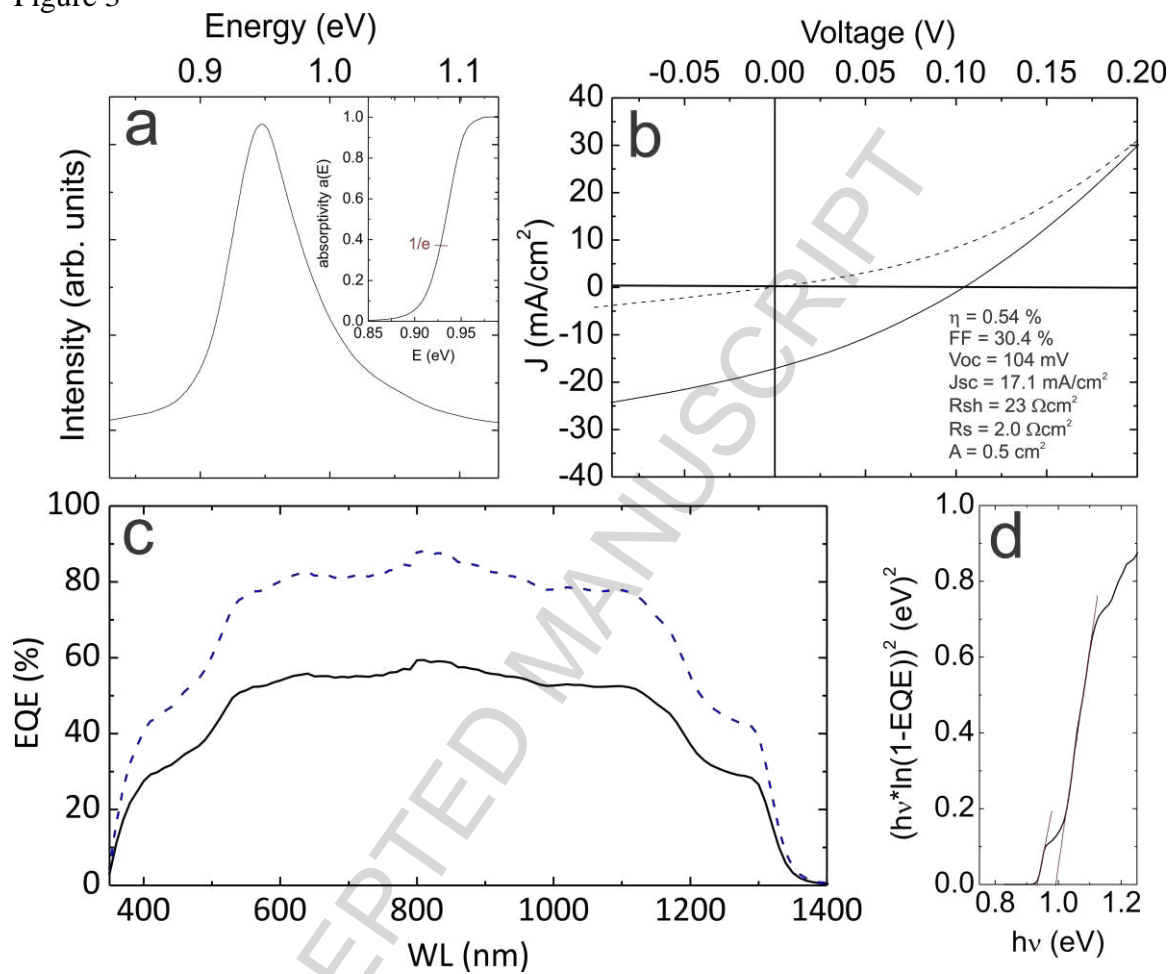
Figures

Figure 1

Figure 2

Figure 3

<u>Highlights</u>

- Fabrication of a pn-junction based thin film solar cell based on Cu2SnS3
- Electro-optical properties of the Cu2SnS3 based solar cell and its limits
- The potential of Cu2SnS3 based solar cells in terms of its photovoltaic application
- Structural, morphological, and optical properties of a Cu2SnS3 thin film